



1

2 **Simulating migration in dynamic** 3 **vegetation models efficiently using** 4 **LPJ-GM**

5

6

7

8 Lehsten, Veike.^{a,b}, Mischurow, Michael.^b, Lindström, Erik.^c, Lehsten, Dörte.^b, Lischke, Heike.^a

9

10 ^a Dynamic Macroecology/ Landscape dynamics, Swiss Federal Institute for Forest, Snow and
11 Landscape Research WSL, Birmensdorf, Switzerland

12 ^b Department of Physical Geography and Ecosystem Science, Lund University, Lund, Sweden

13 ^c Centre for Mathematical Sciences, Department for Mathematics Lund University, Lund, Sweden

14

15

16 ^{*} Corresponding author: veiko.lehsten@gmail.com

17



18 **Abstract**

19 Dynamic vegetation models are a common tool to assess the effect of climate and land use change on
20 vegetation. While the current development aims to include more processes, e.g. the nitrogen cycle, the
21 models still typically assume an ample seed supply allowing all species to establish once the climate
22 conditions are suitable. A number of species have been shown to lag behind in occupying
23 climatological suitable areas (e.g. after a change in the climate) as they need to arrive and establish at
24 the newly suitable areas. Previous attempts to implement migration in dynamic vegetation models
25 have allowed simulating either only small areas or have been implemented as post process, not
26 allowing for feedbacks within the vegetation. Here we present two novel methods simulating
27 migrating and interacting tree species which have the potential to be used for continental simulations.
28 Both distribute seeds between grid cells leading to individual establishment. The first method uses an
29 approach based on Fast Fourier transform while in the second approach we iteratively shift the seed
30 production matrix and disperse seeds with a given probability. While the former method is
31 computationally marginally faster, it does not allow for modification of the seed dispersal kernel
32 parameters with respect to terrain features, which the latter method allows.

33 We evaluate the increase in computational demand of both methods. Since dispersal acts at a scale no
34 larger than 1 km, all dispersal simulations need to be performed at least at that scale. However, with
35 the current available computational power it is not feasible to simulate the vegetation dynamics of a
36 whole continent at that scale. We present an option to decrease the required computational costs,
37 reducing the number of grid cells where the local dynamics is computed by simulating it only along
38 migration transects. Evaluation of species patterns and migration speeds shows that although the
39 simulation along transects reduces the migration speed slightly, both methods are reliable.
40 Furthermore, both methods are sufficiently computationally efficient to allow large scale DGVM
41 simulations with migration on entire continents.

42 **1. Introduction**

43 A large suite of dynamic global vegetation models (DGVMs) is currently used to simulate the effects
44 of climate and / or land use change on vegetation and ecosystem properties. These simulations result
45 in projections (or hind-casts) of species ranges as well as changes in ecosystem properties such as
46 carbon stocks and fluxes. Examples of these DGVMs include ORCHIDEE (Yue et al., 2018), LPJ-
47 GUESS (Sitch et al., 2003), IBIS (Foley et al., 1998), (Sato et al., 2007), for a review of DGVM
48 features see (Quillet et al., 2010).

49 These models typically assume that species can establish at any site once the environmental conditions
50 become suitable. However, in real ecosystems species need not only to establish and replace existing
51 vegetation – the processes gap models describe successfully – but they also need to have sufficient



52 amount of seeds at a given location to successfully establish. Implicitly, current DGVMs assume that
53 ample amounts of seeds of all species are present in every location.

54 While this approach might seem reasonable in cases where the vegetation can keep up with climate
55 change (i.e. moving sufficiently fast to occupy areas which become suitable), there have been a
56 number of instances reported where a considerable migration lag occurred. For instance *Fagus*
57 *sylvatica* has been shown to have a considerable migration lag and is currently still in the process of
58 occupying its climatological optimum (Bradshaw and Lindbladh, 2005).

59 Inclusion of migration is not only of interest to simulate species migration in the past. For the
60 projection of ecosystem properties in the future (with projected climate), migration lags might lead to
61 uncertainties in projected ecosystem properties if the wrong species community is predicted to occur at
62 a certain site. Especially, given that the speed at which environmental conditions change currently is
63 unprecedented at least over the last centuries, effects of the migration lag of key species should be
64 evaluated when projecting ecosystem properties.

65 Migration lags can be caused by different factors. Seed transport might only occur over limited
66 distances. But also low seed amounts and in particular long generation times can slow down
67 migration. Seed amount and generation time depend on the competition with other trees: a free
68 standing tree starts earlier to produce seeds and produces more than a tree of the same age in the
69 closed forest. The competitors, however, are also migrating, which leads to feedbacks between the
70 species.

71 Thus, for simulations over large areas covering long time spans, species migration – consisting of a)
72 local dynamics influenced by the environment, b) competition between species, and c) of seed
73 dispersal – has to be taken into account simultaneously for several species.

74 Species migration has been implemented successfully in dynamic vegetation models working on
75 smaller extents and finer scales than DGVMs typically use, e.g. forest landscape models (FLMs;
76 review in Shifley et al, 2017), such as TreeMig, (Lischke et al., 2006), Landclim (Schumacher *et al.*,
77 2004), Landis (Mladenoff, 2004), or Iland (Seidl et al., 2012).

78 In these models, seed dispersal is modelled in a straightforward way: seeds are distributed from each
79 producing to each receiving cell with a distance dependent probability. However, transferring these
80 approaches to DGVMs is problematic, due to a number of conceptual and technical difficulties.
81 DGVMs usually operate on a coarse spatial resolution to reduce computational load and input data
82 requirements. This neglects the spatial heterogeneity within the grid cells. Additionally, and even more
83 critical for implementing migration, it leads to discretization errors: if it is assumed that the forest
84 representing the grid cell is located in the centre of the cell, the seeds cannot move far enough to leave
85 the cell (given a typical cell size of 50km by 50km). If it is assumed that the simulated forest is



86 uniformly distributed in the cell, with each time step some of the seeds reach the neighbour cell,
87 leading to a resolution dependent speed up of the migration.

88 Additionally specifics of model implementations might complicate the inclusion of migration in some
89 DGVMs. Many DGVM implementations are done in a way that for each grid cell all years are
90 simulated before the simulation of the next cell is started. This is done to minimize input-output effort
91 since the whole climate data for each cell is read in at once and it also eases parallelisation for multi-
92 core computer since in this case each node is assigned a number of grid cells which the node calculates
93 independently of the other nodes with no required communication. However, for simulating seed
94 dispersal, all cells need to be evaluated in each time step.

95 There have been a number of attempts to integrate species migration in DGVMs (cf. Snell *et al.*, 2014,
96 and Discussion section). For example, Sato and Ise (2012) developed a DGVM where species could
97 potentially migrate between neighbouring cells with a fixed rate of about 1km/year.

98 However, to the knowledge of the authors, there is no implementation into a DGVM which allows
99 simulations at continental scale, takes into account the migration within the grid cell and includes
100 feedbacks between all simulated species.

101 Here we present two methods to fill this gap, i.e. allow simulating species migration of several species
102 simultaneously. The methods are implemented into the LPJ-GUESS DGVM but can potentially also
103 be implemented into other DGVMs. Though they are tested here using a virtual landscape they can be
104 applied for continental simulations given current computing resources.

105 **2. Methods**

106 **2.1 The dynamic vegetation model LPJ-GUESS**

107 LPJ-GUESS is a flexible framework for modelling the dynamics of terrestrial ecosystems from
108 landscape to global scales (Sitch *et al.*, 2003; Smith *et al.*, 2001). This DGVM consists of a number of
109 sub-modules containing formulations of subsets of ecosystem processes at defined spatial and
110 temporal scales. A large body of publications describes the features of LPJ-GUESS in detail; here we
111 concentrate on the changes that were applied to LPJ-GUESS version 4.0. To differentiate between the
112 original version of LPJ-GUESS and our extended version (where we implemented the migration
113 module) we refer to the extended version as LPJ-GM (short for LPJ-GUESS-MIGRATION).

114 **2.2 Technical implementation**

115 Standard LPJ-GUESS simulations are typically performed at a computing cluster with cells running on
116 different nodes of the cluster without any interaction of the nodes. We implemented a distributed
117 simulation using MPI (Clarke *et al.*, 1994) with the grid cells communicating with a master process.



118 Seeds are produced potentially in each grid cell at the end of each migration year. The number of seeds
119 produced is sent to the node computing the dispersal while all nodes wait for this node to finish the
120 calculation. This node sends the number of seeds that arrive at each grid cell back to all nodes to
121 continue the calculation.

122 Similar to the standard version of LPJ-GUESS (Sitch et al., 2003; Smith et al., 2001), in the first 100
123 years no seed dispersal is performed and all plant types are allowed to establish and grow without N-
124 limitation to equilibrate the soil pools with carbon and nitrogen. This time period is used to sample
125 NPP given a certain N deposition and climate to subsequently equilibrate the N pools of the soil and a
126 fast spin-up of 40000 years approximated using the sampled rates of C assimilation (Smith et al.,
127 2014). After this initialisation period all vegetation is killed and succession starts from a bare soil and
128 now seed limitation is active.

129 In LPJ-GM seed dispersal is done on an annual basis which corresponds to the temporal resolution of
130 seed production. The amount of seeds produced is communicated to the master node at the end of each
131 year. The master node re-distributes seeds over the whole spatial domain according to the dispersal
132 algorithm and communicates the amounts of arriving seeds back to each grid cell. Seeds transferred to
133 the grid cells are added to the seed bank which determines establishment probability in
134 environmentally-suitable cells. All communications between the processes are done via MPI protocol
135 (Clarke et al., 1994).

136 LPJ-GUESS is a gap model with the typical successional vegetation changes. To even out
137 successional based fluctuations in ecosystem properties and to be able to simulate disturbances a
138 certain number of replicate patches are simulated per grid cell. All patches share the same climate but
139 potentially differ in their successional stage due to different timing of disturbances and stochastic
140 mortality. Conceptually, each patch has a size of 1000 m² but represents an area depending on the
141 resolution of the grid cell. Patches have no spatial position with respect to each other and do not
142 interact (Smith et al., 2001). In LPJ-GM we reduced the number of patches to one but achieved the
143 representative averaging by using explicitly placed small grid cells instead of statistical units (replicate
144 patches). For each large grid cell in the climate grid we simulate a large number of cells of 1km² area
145 resulting in a more than sufficient averaging of successional stages. LPJ-GUESS simulations are
146 typically performed with patch numbers around 10 (e.g. Smith *et al.*, 2001) but depending on the aim
147 of the simulation patch numbers have been increased even to 500 (e.g. Lehsten *et al.*, 2016). In our
148 setup even with 50 km corridors (see below) LPJ-GM represents a 0.5x0.5degree cell with 200
149 simulation cells ranging at the higher end of the patch number per area compared to previous
150 simulations.



151 **2.3 Migration processes**

152 **2.3.1 Seed production**

153 Similar to TreeMig (Lischke et al., 2006) we implemented seed production (depending on leaf area
154 index; LAI) and seed bank dynamics.

155 The seed number produced within each grid cell is calculated as the product of the maximum
156 fecundity multiplied by the proportion of the current LAI to the maximum LAI and multiplied by the
157 area per grid cell (Lischke et al., 2006). No specific age of maturity is taken into account.

158 All seeds of a species produced $S(x', y')$ at a location (x', y') within a year are available for seed
159 dispersal. Once seeds have entered the seed bank, no further dispersal is possible (they remain in the
160 seed bank). Though LPJ-GUESS keeps track of carbon allocated to the main plant compartments and
161 even allocates a certain amount of carbon to seeds (which is transferred to the litter pool, the soil pool
162 and finally the atmosphere), for simplicity we decided not to relate the seed production to the carbon
163 accounting at this point. Allocation rules including seed production and even mast fruiting effects
164 could be included in the future.

165 **2.3.2 Seed dispersal**

166 The produced seeds are distributed according to

$$167 \quad S_d(x, y) = \int S(x', y') k_s(x - x', y - y') dx' dy' \quad (\text{eq. 1}).$$

168 $S(x', y')$ is the seed production, and $k_s(x - x', y - y')$ the seed dispersal kernel in euclidean
169 coordinates. The seed distribution $S_d(x, y)$, i.e. the input of seeds in location x, y is then obtained by
170 integrating over all possible locations x', y' for arriving at x, y .

171 Thus, the seed distribution is given by the convolution of the seed production and the seed dispersal
172 kernel:

$$173 \quad S_d = S ** k_s. \quad (\text{eq. 2})$$

174

175 For this study we used the seed dispersal kernel and parameterization from TreeMig (Lischke *et al.*,
176 2006). The seed dispersal kernel defines the probability of seeds arriving at a sink cell (x, y) from the
177 source cell (x', y') with a certain distance $z = \sqrt{(x - x')^2 + (y - y')^2}$.

178 The kernel is specified in a polar coordinate system,

179 $k_s(z, \theta) = k_s(z|\theta)k_s(\theta)$, with the radial distance z . The seeds follow a mixture of two exponential
180 distributions, the short and the long term dispersal, while the angular dispersion, θ , is uniform in all
181 directions (in our case the angular dispersion θ is uniform, but if one is interested in implementing
182 wind directions this can be changed). Thus, the radial component of the kernel is given by



$$183 \quad k_s(z|\theta) = (1 - \kappa) \frac{1}{\alpha_{s,1}} e^{-\frac{z}{\alpha_{s,1}}} + \kappa \frac{1}{\alpha_{s,2}} e^{-\frac{z}{\alpha_{s,2}}}, \kappa \in (0,1) \quad (\text{eq. 3})$$

184 while the angular term is given by

$$185 \quad k_s(\theta) = \frac{1}{2\pi} 1_{\{\theta \in [0, 2\pi]\}}. \quad (\text{eq. 4})$$

186 The dispersal kernel is defined by the species specific values for the proportion of long term dispersal
 187 κ and the species expected dispersal distances $\alpha_{s,1}$ and $\alpha_{s,2}$ for the two kernels.

188 The species specific values for these parameters were roughly estimated by Lischke *et al.* (2006) to be
 189 0.99 for κ_s and 25m and 200m for the two mean dispersal distances k_s for *Fagus sylvatica*.

190 **2.3.3 Seed bank dynamics**

191 The number of the seeds in the seed bank is increased by the influx S_d of seeds according to (eq. 1),
 192 and reduced by the yearly loss of germinability and the amount of germinated seeds at the end of each
 193 simulated year, similar to TreeMig (Lischke et al., 2006).

194 A year is defined for each species and grid cell before which seed bank constraints are ignored (hence
 195 free establishment happens). This way we can specify in which areas each species is already
 196 potentially established at the beginning of the simulation and this defines thereby the location of the
 197 refugia. This parameter can also indicate that a species is not hindered in its establishment by
 198 migration.

199 **2.3.4 Germination**

200 LPJ-GUESS is a gap model and in the original version the number of newly established saplings only
 201 depends on the amount of light reaching the forest floor (given that the cell has a suitable climate). In
 202 LPG-GM we additionally limit the establishment of seedlings depending stochastically depending on
 203 the number of available seeds. The probability that a species establishes is proportional to the seed
 204 number in the seed bank multiplied by the seed germination proportion and an extra parameter which
 205 (implicitly) takes the area of each grid cell into account. In our case we fixed this parameter to 0.01
 206 after initial testing. Hence if in a certain year 100 seeds are in the seed bank per and the germination
 207 rate is 0.71 (value for *Fagus sylvatica*) the probability of an age cohort establishing is
 208 $0.01 * 100 * 0.71 = 0.71$.

209 **2.4 Enhanced dispersal simulation**

210 One way to simulate seed dispersal is to calculate the convolution of all seeds produced of the matrix
 211 containing the seed production and the seed dispersal kernel (specified in eq. 1 and eq. 3). However,
 212 evaluating the convolution explicitly can be computationally expensive for seed dispersal kernels with
 213 long range.



214 **2.4.1 Fast Fourier transformation method (FFTM)**

215 An alternative is based on the convolution theorem and the Fast Fourier Transformation (FFT), a
216 technique commonly used in physics, image processing and engineering (Strang, 1994).

217 This approach carries out the computations in the frequency domain, see Gonzales & Woods (2002).

218 Here we use the notation $F\{S\} = \int e^{-iux-ivy} S(x, y) dx dy$ to denote the two dimensional Fourier
219 transform of S and correspondingly $F\{k_s\}$ the two dimensional Fourier transform of k_s . It then follows
220 that the Fourier transform of the convolution equals the product of the Fourier transforms

221
$$F\{S ** k_s\} = F\{S\}F\{k_s\} \quad (\text{eq. 5})$$

222 Thus, it is possible to compute the convolution by applying the inverse Fourier transform to the
223 products of the Fourier transforms

224
$$S ** k_s = F^{-1}\{F\{S\}F\{k_s\}\} \quad (\text{eq. 6})$$

225 This equation must be discretized before evaluating it on a computer. The discrete Fourier transform is
226 computed using the Fast Fourier Transform (Cooley and Tukey, 1965), which has a computational
227 cost of $O(N^2 \log^2(N))$ in two dimensions. The discrete approximation of S_d is then given by

228
$$S_d = F^{-1}\{F\{S\} \odot F\{k_s\}\} \quad (\text{eq. 7})$$

229 where \odot is the element-wise (Hadamard product) multiplication of matrices.

230 Nowadays, software packages for FFT typically only compute positive frequencies. That means that
231 we have to shift the frequencies prior to the element-wise multiplication of $F\{S\}$ and $F\{k_s\}$. This is
232 illustrated in Fig.1 see also supplementary material S.2.

233

234 <Figure 1 to be placed here>

235 While this method allows including different wind distributions by changing the seed dispersal kernel,
236 it does not allow to use different seed dispersal kernels at different locations, e.g. due to prevailing
237 wind directions in valleys, due to barriers to animal transport like a motorway, or due to lower
238 transport permeability in already forested areas.

239 **2.4.2 Seed matrix shifting method (SMSM)**

240 Another way to simulate seed dispersal is to simulate the seed movement between the cells explicitly
241 by shifting the matrix containing the produced seeds by one position (repeatedly in all directions of the
242 Moore neighbourhood) and simulating seed transport of a certain proportion of the seeds into the next
243 cell. Each move can be viewed as an independent random variable. Repeating these moves thus



244 corresponds to a random walk process. The Lindeberg's condition for sequences for sums of
245 independent random variables ensures that the kernel will be Gaussian under general conditions
246 (Shiryayev, 2016), with the expected value given by the sum of expected values for each random
247 variable and similarly for the variance (see supplementary material S.1 for a formal proof and a
248 derivation of the parameters of the resulting normal distribution).

249 If this is done repeatedly it allows an easy implementation of spatial explicit differences in seed
250 dispersal kernel distributions, by adjusting the proportions of seeds being transported into the next cell
251 according to a similarly sized matrix containing the area roughness or permeability. By this approach,
252 barriers and even wind speeds in latitudinal and longitudinal directions can be implemented by
253 adjusting the dispersal probabilities accordingly.

254

255 <Figure 2 placed here>

256 After the distribution of the dispersed seeds is calculated, the seeds are added to the seed bank.

257 **2.5 Corridors**

258 Seed dispersal acts at a rather fine scale compared to the usual scale at which DGVMs are run (LPJ-
259 GUESS is typically run at a 0.5 to 0.1 degree longitude / latitude scale). Given that the average long
260 distance seed dispersal for example for *Fagus sylvatica* is 200 m, simulations at such a coarse scale
261 will not be able to capture this process.

262 As a compromise between currently available computing resources and required simulation detail we
263 choose a 1km scale at which we performed our simulations. However, even at this scale, simulating
264 for example the European continent would result in an extreme computational effort.

265 Given that in some areas the landscape is rather homogenous while other areas have a variable terrain
266 (or land use conditions), we test whether for the homogenous landscapes it is sufficient to simulate the
267 local dynamics only in latitudinal, longitudinal and diagonal transects (corridors) and how this will
268 influence the migration speed. The corridors are 1 grid cell wide and regularly placed in the simulation
269 domain. Their density can be chosen by defining the distance between the latitudinal and longitudinal
270 corridors.

271 Although LPJ-GM only simulates local dynamics in the cells along the corridors, the seed matrix
272 needed to be filled for the dispersal calculation using the FFTM or the SMSM algorithm. We applied a
273 nearest neighbour interpolation of the seed production before performing the seed dispersal calculation
274 (theoretical considerations show that a distance weighted average would strongly speed up the
275 migration).



276 **2.6 Simulation experiments**

277 To test our newly developed migration module we simulated the spread of a single late successional
278 species (*Fagus sylvatica*) through an area covered by an early successional species (*Betula pendula*).
279 All grid cells and all years in the simulated area had a static climate suitable for both species. For a
280 specific simulation using the SMSM method we assumed differences in the dispersal ability (e.g. more
281 or less permeable areas or physical barriers) while the climate on all grid cells is still static and
282 favourable. Given the uniformity of the climate, there should be no variability in the migration speed
283 caused by differences in climatic conditions. We simulated the spread of *F. sylvatica* from a single
284 grid cell in the corner of the study area which represents the refugium. We tested several corridor
285 distances (between the parallel and between the diagonal corridors) for their effect on the migration
286 speed. We calculated the migration speed as the distance between the start point of the migration and
287 the 95 percentile farthest point in the virtual landscape where the leaf area index (LAI) of *F. sylvatica*
288 is larger than 0.5 divided by the simulated time elapsed since the start of the migration. To avoid
289 founder effects we neglected the points within the first 5 km of the refugium. The simulations were
290 performed over 3000 years and over an area of 100 by 100 cells of 1 km². Finally we ran one
291 simulation where we did not calculate the seed dispersal (but performed all communication between
292 cells), hence allowing us to estimate the computation time demand for the seed dispersal calculation.

293 **3. Results**

294 **3.1 Explicit seed dispersal**

295 Pre-studies have shown that both the FFTM as well as the SMSM are performing much faster than an
296 explicit dispersal from each grid cell to each other within the range of the dispersal. This is especially
297 pronounced if the area to be simulated is increased. Instead of comparing the explicit seed exchange
298 with the FFTM using LPJ-GM we demonstrated this with a small Matlab™ script in the
299 supplementary material S.2 which also allows demonstrating both the transformation of the seed
300 dispersal kernel as well as the FFTM in detail.

301 **3.2 FFTM simulations**

302 Using the parameterization from TreeMig in a complete (no corridors) simulation area of 100 by 100
303 grid cells results in a migration speed of 34 m per year for *Fagus sylvatica* (Fig. 3).

304 <Figure 3 placed here>

305 Though the establishment is stochastic, the spread is relatively smooth. Using at a distance of 10 km,
306 20 km and 50 km results in a somewhat reduced migration rate of 26, 28 and 28 m/year (compared to
307 a simulation without corridors), respectively (Fig 3, lower three rows of panels). While in the
308 simulation without corridors the variability of the migration speed is relatively low (dots under the red
309 line in upper left panel of Fig 3), this variability is strongly increased when corridors are simulated.



310 This is caused by *F. sylvatica* migrating along the diagonal, reaching the end point of the diagonal and
311 then migrating along the longitudinal and latitudinal corridors into cells which have actually a shorter
312 distance to the refugia than the endpoint of the diagonal.

313 The calculation time per grid cell in the whole area (range for which the seed dispersal is computed) is
314 increased by 12% by simulating the FFT, but by using the corridors it is reduced to 36%, 22% and
315 12%, compared to simulating the full area (Tab. 1, col. 7). The proportion of computation time used
316 to perform the FFT increases from 11% without corridors to 18%, 29% and 29% for simulations with
317 corridors every 10, 20 and 50 km. This estimate only includes the required time for computing the
318 FFT-based seed dispersal since the control run without seed dispersal still contained all
319 communication between cells. For the control run seeds were produced and sent to the master but the
320 master did not compute the seed dispersal, though still communicated with all other nodes to allow a
321 fair assessment of the computation time demand of the two methods (see Tab. 1).

322 3.3 Shifting seed simulations

323 Initial testing of the probability parameter for the SMSM suggested a value of $p=5 \cdot 10^{-7}$ to generate a
324 migration speed comparable to the migration speed for the FFTM based on the TreeMig
325 parameterization.

326 This resulted in a migration speed of 39 m/year for the filled area and 27m/year respective 29 m/year
327 and 30m/year for the 10 km, 20 km and 50km corridors (Fig. 4).

328 <Figure 4 placed here>

329 Similarly to the FFTM simulations, the migration speed is reduced (see table 1 for a summary). Also
330 comparable to the FFTM based seed dispersal computation, calculation time per grid cell in the whole
331 area (range for which the seed dispersal is computed) is increased by 16% by the simulation of
332 dispersal, but reduced to 35%, 19% and 11% by using the corridors. The proportion of calculation
333 time spend for simulating the seed dispersal is comparable to the proportion using the FFT, it is 16%,
334 19%, close to 23% and 32% (see Tab. 1).

335 Since the SMSM allows adjusting the probability depending on the seed transport permeability of the
336 terrain we also simulated the migration within a non-homogenous dispersal area. The results of this
337 simulation are displayed in Fig 5.

338

339 <Figure 5 placed here>

340 Though all cells of the virtual landscape have a similar climate, some cells will never be occupied (see
341 Fig. 5) because the seeds are not able to reach them (which might not be reasonable for real world



342 simulations but demonstrates the method). Migration speed is different in different parts of the
343 simulated area.

344 <Table 1 placed here>

345



346 **4. Discussion**

347 To our knowledge we are the first that manage to implement (tree-) species migration in a DGVM in a
348 way that allows continental simulations of simultaneously migrating and interacting species.

349 **4.1 Performance of new migration methods**

350 The presented new methods for simulating migration in DGVMs show a promising performance in
351 different aspects.

352 The first is the gain of efficiency by the FFTM and the SMSM methods as compared to the traditional,
353 straightforward approach to evaluate the seed transport from each cell to each other (last Fig in S.2). A
354 two dimensional FFT can be obtained by successive passes of the one dimensional FFT, hence the
355 complexity will be the one-dimensional complexity squared (Gonzalez and Woods, 2002). The
356 computational complexity for the FFTM is $O(N^2 \log^2(N))$ for a $N \times N$ grid discretizing the seed
357 distribution, while the complexity of the direct implementation of the convolution approach in the
358 SMSM is $O(2KRN^2)$ for a $N \times N$ grid discretizing the seed distribution and $R \times R$ kernel (for the
359 derivation see supplementary material S.1). This can be computationally comparable to the FFTM for
360 kernels with short range of R . Secondly, simulating the local dynamics only along the corridors
361 instead of in the full area resulted in a very similar migration pattern, and the simulated migration
362 speed is similar to that of the simulation with full grid cell cover (it is slightly slower, caused by the
363 stochasticity of the establishment), but needs much less computing time (reduction of 88% for the
364 corridors every 50km).

365 **4.2 Comparison of the two dispersal methods**

366 In this study we present two alternative methods for simulating dispersal, which differ in their
367 properties. While the FFTM allows any type of seed dispersal kernel, the SMSM corresponds to a
368 normal distribution kernel. Although other shapes of dispersal kernels can be approximated by
369 weighted sums of normal distributions, of which each of them has to be simulated by an own SMSM,
370 which will cause strong increases in computational demand.

371 On the other hand, the advantage of the SMSM lies in its ability (contrary to the FFTM) to modify the
372 parameters of the seed dispersal kernel spatially depending on the terrain. If instead of applying a
373 single permeability for all directions, different permeability is applied for each of the 8 directions (e.g.
374 north, northeast, east, etc.) this method also allows a spatially explicit consideration of wind directions
375 (which is not possible for the FFTM, as it relies on a universal kernel applied to the whole entire area).
376 Hence, depending on the aim of the analysis either one of the algorithms most suitable.

377 **4.3 Comparison to other approaches**

378 Our new species migration submodule FFTM uses for the first time (to our best knowledge) in ecology
379 an algorithm based on Fast Fourier Transformation to simulate dispersal in a DGVM, which due to its



380 efficiency is one of the “workhorses” in mathematics, physics and signal processing (Strang, 1994).
381 The SMSM, in turn, mimics the seed transport process itself in a simple and straightforward way,
382 which to our knowledge has also not been implemented in DGVMs either.

383 Both approaches are combined with features of modelling species migration that are already used in
384 other DGVMs (cf. Snell, 2014).

385 The cellular automaton KISSMig (Nobis & Normand, 2014), e.g. simulates the spread of single
386 species driven by a spatio-temporal grid of suitability, and by transitions to the nearest neighbour cells,
387 which is similar to one iteration in the SMSM. The suitability based models CATS (Dullinger *et al.*,
388 2012) or MigClim (Engler and Guisan, 2009) simulate a simple demography of single species and
389 explicitly the spread based on a seed dispersal kernel.

390 To also account for ecophysiology, the CATS model was combined with LPJ-GUESS in a post-
391 processing approach (Lehsten *et al.*, 2014) which used a spatio-temporally explicit suitability
392 estimated from LPJ-GUESS simulated productivity of a single species, assuming the presence of the
393 other species. This suitability was subsequently used within CATS to simulate migration spread rates.
394 Such a post-processing approach however does not include interactions between several migrating
395 species.

396 Forest landscape models have been developed to integrate such feedbacks between species as well as
397 dispersal (He *et al.*, 2017; Shifley *et al.*, 2017). These models simulate local vegetation dynamics with
398 species interactions, and dispersal by explicit calculation of seed or seedling transport probabilities
399 with dispersal kernels of different shapes (e.g. LandClim (Schumacher *et al.*, 2004), Landis
400 (Mladenoff, 2004), Iland (Seidl *et al.*, 2012)). To capture spatial heterogeneity, they run at a
401 comparably fine spatial resolution (about 20-100m grid cells), allowing only the simulation of
402 relatively small areas due to computational demands.

403 To overcome such computational limits, several approaches for a spatial upscaling of the models have
404 been put forward. For example, the forest landscape model TreeMig can operate at a coarser resolution
405 (grid cell size 1000m) because it aggregates the within-stand- heterogeneity by dynamic distributions
406 and height classes (Lischke *et al.*, 1998), which allows applications at a larger scale, e.g. over entire
407 Switzerland (Bugmann *et al.*, 2014) or on a transect through Siberia (Epstein *et al.*, 2007). Another
408 upscaling of TreeMig was achieved by the D2C method (Nabel, 2015; Nabel and Lischke, 2013)
409 which simulates local vegetation dynamics only in a subset of cells that are dynamically determined as
410 representative for classes of similar cells. This method led to a computing time reduction of 30-85% as
411 compared to the full simulation similar to our transect methods which resulted in 85 % gain of
412 computing time.



413 In dynamic global vegetation models (DGVMs), the discretization problem is even more pronounced,
414 because they are designed to operate on very large extents (continents or the entire globe). Given the
415 computational demands of the simulations, they are therefore typically running at a coarse resolution
416 for example 0.5 or 0.1 degree longitude / latitude, and simulate the vegetation dynamics at the centre
417 of each of these grid cells, assuming this point to be representative for the entire cell.

418 Snell (2014) approached the discretization problem for the DGVM LPJ-GUESS by also using a
419 reduced number of representative units (here patches) within each grid cell. She assumed that the
420 numerous replicates of the vegetation dynamics on a patch are randomly distributed over the area of
421 the grid cell. Migration within the grid cell is treated similar to an infection process, where the
422 probability of a patch becoming infected (e.g. of the migrating species being able to establish) depends
423 only on the number of already invaded patches within the grid cell. Only once a migrating species
424 managed to establish in a certain proportion of the patches of the simulated grid cell, further dispersal
425 (explicit via a dispersal kernel) into surrounding grid cells is possible. Yet, there is no spatial
426 orientation of the patches within the grid cell and all simulations in this approach are strongly
427 resolution dependent. Simulations of large areas such as continents remain computational challenging
428 with this approach.

429 Our transect approach, similarly to the approach of Snell (2014), uses smaller representative spatial
430 units, 1km-cells, for a spatial upscaling. Since these small grid cells are arranged in contiguous
431 corridors, the migration along these corridors can be simulated without or with only a small
432 discretization error. The results indicate that also the error potentially introduced by the interpolation
433 to the rest of the area is small.

434 Thus, with our approaches, we have combined several advantages of the before mentioned approaches:
435 the seed dispersal from forest landscape models, improved by the novel FFTM or SMSM and the
436 ecophysiology, structure and community dynamics of LPJ-GUESS. We furthermore found a
437 compromise between discretization and efficiency by the corridor method.

438 **4.4 Potential further improvements**

439 Despite the satisfying performance of the new methods in these first tests some aspects suggest further
440 development.

441 **4.4.1 Computation time**

442 Even with the computing time reduction by the corridor approach using a corridor of 50km distance,
443 the computing time required for the simulations including dispersal is still considerable. This is caused
444 by the number of cells on the corridors where the local dynamics is simulated being larger than the
445 number of replicates usually used in all the 1 or 0.5 degree grid cells simulated in traditional DGVMs.
446 For large-scale applications, the approach should be further optimized, e.g. by choosing corridors
447 even further apart from each other in homogenous areas and adapting the corridor density to the large



448 scale (between grid-cell) heterogeneity of the terrain. The within grid-cell heterogeneity in turn can be
449 accounted for by deriving seed dispersal permeability, that can be used in the SMSM approach.
450 Another area of improvement lies in the technical implementation of the seed dispersal algorithm. In
451 the current implementation the seed dispersal is performed at a single cpu, while all other cpus wait
452 until they receive the seeds. There are certainly ways to perform the seed dispersal computation on
453 several nodes to decrease the waiting time. Furthermore, in multi-species simulations the dispersal has
454 to be calculated for each migrating species. In this case, the dispersal of different species should be
455 calculated on separate nodes. When evaluating the run times needed for the simulated areas in the
456 supplementary material it becomes obvious that sometimes larger areas resulted in shorter runtimes for
457 the FTTM (last Fig. in S.2). The differences are quite pronounced given that the time axis is
458 logarithmic. These decreases are caused by the effect that the calculation of a fft can be optimised in
459 case the domain has a size of 2^n .

460 **4.4.2 Migration speed reduction by corridor approach**

461 As expected, any sub-cell assumption results in discretisation errors. In our case the assumption of a
462 corridor slightly reduced the migration speed. This needs to be taken into account when evaluating the
463 result of such studies. The design of the corridors might also not be optimal, maybe a corridor wider
464 than a single cell might result in less decrease of migration speed. However, these types of analysis are
465 outside the scope of this study.

466 **4.4.3 Parameterisation of dispersal kernels**

467 In this study the focus is on developing and testing the novel methods, i.e. we do not attempt to
468 correctly simulate the spread of *F. sylvatica* over a defined time period. The calculated spread rates are
469 well below most of the spread rates in the literature. *F. sylvatica* has been estimated to migrate with ca
470 100 m per year based on pollen analyses by Bradshaw and Lindbladh (2005). Although such estimated
471 high migration speeds could also be the result of glacial refugia located further north than assumed
472 (Feurdean et al., 2013), our estimates of the migration speeds of 20-30 m/year still seem rather low.
473 However, in this paper we aimed to implement tree migration by using the parameterisation of
474 TreeMig in a DGVM and thereby allow continental scale simulations. Our estimated migration rates
475 of 20-30 m per year are very close to the migration rates estimated for this parameterisation for
476 TreeMig by Meier *et al.*, (2012) which estimated a value of 22 m per year. Hence, though we
477 implemented the migration module into a conceptually very different model, the resulting migration
478 rate remains comparably similar.

479 To perform modelling runs estimating the migration speed of any species would require a fine tuning
480 of the seed production and dispersal parameters (which are both very rough estimates in TreeMig
481 (Lischke et al., 2006) to generate the observed migration e.g. by comparing to migration rates based on
482 pollen records.



483 **4.5 Potential for applications**

484 The test simulations were performed at a virtual landscape of 100km by 100km, but eventually the
485 method is aimed to allow continental simulations over several millennia. Regarding memory
486 requirements, this is possible of currently available hardware: Test runs with landscapes of 4000 by
487 4000 grid cells (i.e. the size of Europe) performed without technical problems at least regarding the
488 memory requirement (given 62 GB of RAM). The considerable computational costs however require a
489 relatively high amounts of computing time, which might be reduced by efforts for speeding up (due to
490 efficient parallelisation) of the FFT as the local simulations, e.g. by even further apart corridors.

491 **5. Conclusions**

492 The presented novel approaches offer a high potential to simulate the spatiotemporal dynamics of
493 species which are migrating and interacting with each other simultaneously. The approaches are not
494 restricted to LPJ-GUESS, but can in principle be applied to other DGVMs or FLMs which simulate
495 seed (or seedling) production and explicit regeneration. While the presented methods will allow in
496 future to simulate tree migration at continental scale and over paleo time scales, our study also shows
497 that the estimates for seed dispersal kernels for the major tree species need to be revised to allow truly
498 mechanistic simulations of forest development for example over the Holocene.

499 **6. Author contributions**

500 VL, DL and HL designed the study, VL performed the simulations and the statistical analysis. MM
501 and EL contributed to the study design, MM also performed large parts of the coding. EL developed
502 the formal proof in Supplementary material S.1 and the computation performance related estimates the
503 Conclusion section. All authors contributed to the writing of the article.

504 **7. Competing interests**

505 The authors declare that they have no conflict of interest.

506 **8. Acknowledgements**

507 This study was funded by the Swiss National Science Foundation project CompMig, Nr .
508 205321_163223 .

509 **9. Code and Data availability**

510 The code generating the figures in Supplementary material 2 are part of the material. The used DGVM
511 LPJ-GUESS containing the migration module can be requested from the author.



512 The data behind all figures will be published on the DataGURU server (dataguru.lu.se) with an own
513 DOI upon acceptance of the paper.

514 **10. References**

515

516 Bradshaw, R. H. W. and Lindbladh, M.: Regional spread and stand-scale establishment of *Fagus*
517 *sylvatica* and *Picea abies* in Scandinavia, *Ecology*, 86(7), 1679–1686, doi:10.1890/03-0785, 2005.

518 Bugmann, H. K. M., Brang, P., Elkin, C., Henne, P., Jakoby, O., Lévesque, M., Lischke, H., Psomas,
519 A., Rigling, A., Wermelinger, B. and Zimmermann, N. E.: Climate change impacts on tree species,
520 forest properties, and ecosystem services, in CH2014-Impacts (2014): Toward Quantitative Scenarios
521 of Climate Change Impacts in Switzerland, edited by O. (Meteoswiss) Foen., 2014.

522 Clarke, L., Glendinning, I. and Hempel, R.: The MPI Message Passing Interface Standard, in
523 Programming Environments for Massively Parallel Distributed Systems, edited by R. R. . Decker
524 K.M., Birkhäuser, Basel., 1994.

525 Cooley, J. W. and Tukey, J. W.: An Algorithm for the Machine Calculation of Complex Fourier Series
526 Mathematics of Computation An Algorithm for the Machine Calculation of Complex Fourier Series,
527 Source Math. Comput., 19(90), 297–301, doi:10.2307/2003354, 1965.

528 Dullinger, S., Willner, W., Plutzer, C., Englisch, T., Schrott-Ehrendorfer, L., Moser, D., Ertl, S., Essl,
529 F. and Niklfeld, H.: Post-glacial migration lag restricts range filling of plants in the European Alps,
530 Glob. Ecol. Biogeogr., 21(8), 829–840, doi:10.1111/j.1466-8238.2011.00732.x, 2012.

531 Engler, R. and Guisan, A.: MigClim: Predicting plant distribution and dispersal in a changing climate,
532 Divers. Distrib., 15(4), 590–601, doi:10.1111/j.1472-4642.2009.00566.x, 2009.

533 Epstein, H. E., Yu, Q. Y. Q., Kaplan, J. O. and Lischke, H.: Simulating Future Changes in Arctic and
534 Subarctic Vegetation, *Comput. Sci. Eng.*, 9(4), 12–23, doi:10.1109/MCSE.2007.84, 2007.

535 Feurdean, A., Bhagwat, S. A., Willis, K. J., Birks, H. J. B., Lischke, H. and Hickler, T.: Tree
536 Migration-Rates: Narrowing the Gap between Inferred Post-Glacial Rates and Projected Rates, *PLoS*
537 *One*, 8(8), doi:10.1371/journal.pone.0071797, 2013.

538 Foley, J. A., Levis, S., Prentice, I. C., Pollard, D. and Thompson, S. L.: Coupling dynamic models of
539 climate and vegetation, *Glob. Chang. Biol.*, 4(5), 561–579, doi:10.1046/j.1365-2486.1998.00168.x,
540 1998.

541 Gonzalez, R. C. and Woods, R. E.: Digital Image Processing, 2nd ed., Prentice Hall., 2002.



- 542 He, H. S., Gustafson, E. J. and Lischke, H.: Modeling forest landscapes in a changing climate: theory
543 and application, *Landsc. Ecol.*, 32(7), 1299–1305, doi:10.1007/s10980-017-0529-4, 2017.
- 544 Lehsten, D., Dullinger, S., Huber, K., Schurgers, G., Cheddadi, R., Laborde, H., Lehsten, V., Francois,
545 L., Dury, M. and Sykes, M. T.: Modelling the Holocene migrational dynamics of *Fagus sylvatica* L.
546 and *Picea abies* (L.) H. Karst, *Glob. Ecol. Biogeogr.*, 23(6), 658–668, doi:10.1111/geb.12145, 2014.
- 547 Lehsten, V., Arneith, A., Spessa, A., Thonicke, K. and Moustakas, A.: The effect of fire on tree-grass
548 coexistence in savannas: A simulation study, *Int. J. Wildl. Fire*, 25(2), doi:10.1071/WF14205, 2016.
- 549 Lischke, H., Löffler, T. J. and Fischlin, A.: Aggregation of individual trees and patches in forest
550 succession models: Capturing variability with height structured, random, spatial distributions, *Theor.*
551 *Popul. Biol.*, 54(3), 213–226, doi:10.1006/tpbi.1998.1378, 1998.
- 552 Lischke, H., Zimmermann, N. E., Bolliger, J., Rickebusch, S. and Löffler, T. J.: TreeMig: A forest-
553 landscape model for simulating spatio-temporal patterns from stand to landscape scale, *Ecol. Modell.*,
554 199(4), 409–420, doi:10.1016/j.ecolmodel.2005.11.046, 2006.
- 555 Meier, E. S., Lischke, H., Schmatz, D. R. and Zimmermann, N. E.: Climate, competition and
556 connectivity affect future migration and ranges of European trees, *Glob. Ecol. Biogeogr.*, 21(2), 164–
557 178, doi:10.1111/j.1466-8238.2011.00669.x, 2012.
- 558 Mladenoff, D. J.: LANDIS and forest landscape models, *Ecol. Modell.*, 180(1), 7–19,
559 doi:10.1016/j.ecolmodel.2004.03.016, 2004.
- 560 Nabel, J. E. M. S.: Upscaling with the dynamic two-layer classification concept (D2C): TreeMig-2L,
561 an efficient implementation of the forest-landscape model TreeMig, *Geosci. Model Dev.*, 8(11), 3563–
562 3577, doi:10.5194/gmd-8-3563-2015, 2015.
- 563 Nabel, J. E. M. S. and Lischke, H.: Upscaling of spatially explicit and linked time- and space-discrete
564 models simulating vegetation dynamics under climate change., in 27th International Conference on
565 Environmental Informatics for Environmental Protection, Sustainable Development and Risk
566 Management, *EnviroInfo 2013*, edited by B. Page, F. A. G. J. Göbel, and V. Wohlgemuth, pp. 842–
567 850, Hamburg., 2013.
- 568 Nobis, M. P. and Normand, S.: KISSMig - a simple model for R to account for limited migration in
569 analyses of species distributions, *Ecography (Cop.)*, 37(12), 1282–1287, doi:10.1111/ecog.00930,
570 2014.
- 571 Quillet, A., Peng, C. and Garneau, M.: Toward dynamic global vegetation models for simulating
572 vegetation–climate interactions and feedbacks: recent developments, limitations, and future



- 573 challenges, *Environ. Rev.*, 18(NA), 333–353, doi:10.1139/A10-016, 2010.
- 574 Sato, H. and Ise, T.: Effect of plant dynamic processes on African vegetation responses to climate
575 change: Analysis using the spatially explicit individual-based dynamic global vegetation model
576 (SEIB-DGVM), *J. Geophys. Res.*, 117(G3), G03017, doi:10.1029/2012JG002056, 2012.
- 577 Sato, H., Itoh, A. and Kohyama, T.: SEIB-DGVM: A new Dynamic Global Vegetation Model using a
578 spatially explicit individual-based approach, *Ecol. Modell.*, 200(3–4), 279–307,
579 doi:10.1016/j.ecolmodel.2006.09.006, 2007.
- 580 Schumacher, S., Bugmann, H. and Mladenoff, D. J.: Improving the formulation of tree growth and
581 succession in a spatially explicit landscape model, *Ecol. Modell.*, 180(1), 175–194,
582 doi:10.1016/j.ecolmodel.2003.12.055, 2004.
- 583 Seidl, R., Rammer, W., Scheller, R. M. and Spies, T. A.: An individual-based process model to
584 simulate landscape-scale forest ecosystem dynamics, *Ecol. Modell.*, 231, 87–100,
585 doi:10.1016/j.ecolmodel.2012.02.015, 2012.
- 586 Shifley, S. R., He, H. S., Lischke, H., Wang, W. J., Jin, W., Gustafson, E. J., Thompson, J. R.,
587 Thompson, F. R., Dijak, W. D. and Yang, J.: The past and future of modeling forest dynamics: from
588 growth and yield curves to forest landscape models, *Landsc. Ecol.*, 32(7), 1307–1325,
589 doi:10.1007/s10980-017-0540-9, 2017.
- 590 Shiryaev, A. N.: *Probability*, 3rd ed., Springer Verlag, New York., 2016.
- 591 Sitch, S., Smith, B., Prentice, I. C., Arneth, A., Bondeau, A., Cramer, W., Kaplan, J. O., Levis, S.,
592 Lucht, W., Sykes, M. T., Thonicke, K. and Venevsky, S.: Evaluation of ecosystem dynamics, plant
593 geography and terrestrial carbon cycling in the LPJ dynamic global vegetation model, *Glob. Chang.*
594 *Biol.*, 9(2), 161–185, 2003.
- 595 Smith, B., Prentice, I. C. and Sykes, M. T.: Representation of vegetation dynamics in the modelling of
596 terrestrial ecosystems: comparing two contrasting approaches within European climate space, *Glob.*
597 *Ecol. Biogeogr.*, 10(6), 621–637, 2001.
- 598 Smith, B., Wärlind, D., Arneth, A., Hickler, T., Leadley, P., Siltberg, J. and Zaehle, S.: Implications of
599 incorporating N cycling and N limitations on primary production in an individual-based dynamic
600 vegetation model, *Biogeosciences*, 11(7), 2027–2054, doi:10.5194/bg-11-2027-2014, 2014.
- 601 Snell, R. S.: Simulating long-distance seed dispersal in a dynamic vegetation model, *Glob. Ecol.*
602 *Biogeogr.*, 23(1), 89–98, doi:10.1111/geb.12106, 2014.
- 603 Snell, R. S., Huth, A., Nabel, J. E. M. S., Bocedi, G., Travis, J. M. J., Gravel, D., Bugmann, H.,



- 604 Gutiérrez, A. G., Hickler, T., Higgins, S. I., Reineking, B., Scherstjanoi, M., Zurbriggen, N. and
605 Lischke, H.: Using dynamic vegetation models to simulate plant range shifts, *Ecography (Cop.)*,
606 37(12), 1184–1197, doi:10.1111/ecog.00580, 2014.
- 607 Strang, G.: Wavelets, *Am. Sci.*, 82(May-June), 250–255, 1994.
- 608 Yue, C., Ciais, P., Luyssaert, S., Li, W., McGrath, M. J., Chang, J. and Peng, S.: Representing
609 anthropogenic gross land use change, wood harvest, and forest age dynamics in a global vegetation
610 model ORCHIDEE-MICT v8.4.2, *Geosci. Model Dev.*, 11(1), 409–428, doi:10.5194/gmd-11-409-
611 2018, 2018.
- 612

613 **10. Contents of the supplementary material**

614

- 615 Derivation of the variance of the seed dispersal kernel for the SMSM S.1
- 616 Example evaluation of computation time difference between FFTM and the
617 traditional method S.2
- 618 In this appendix an example code for the FFTM is given together
619 with code demonstrating the required transformation of the seed
620 kernel for the FFTM

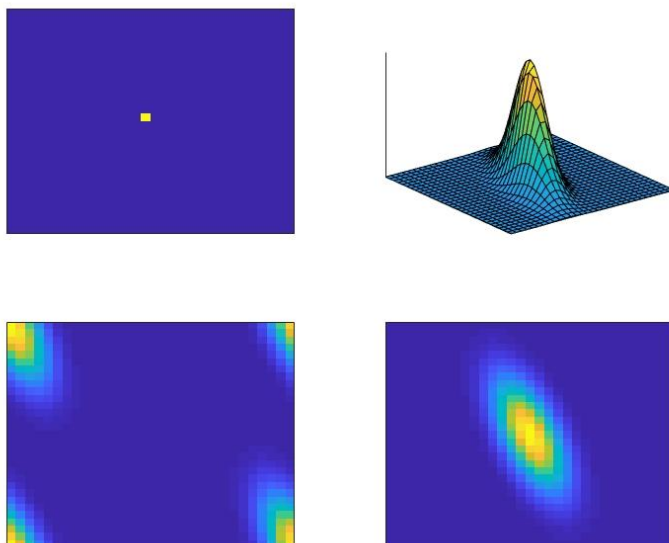
621

622



623 **11. Figures and tables**

624
625



626

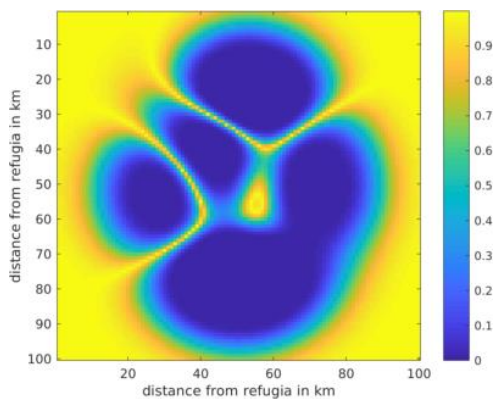
627 Fig. 1. Upper left panel: seed source. Upper right panel: example of a seed dispersal kernel (here a
628 non-symmetric kernel is assumed), lower left panel: transformed seed dispersal kernel, lower right
629 panel: seed distribution after convolution.

630



631

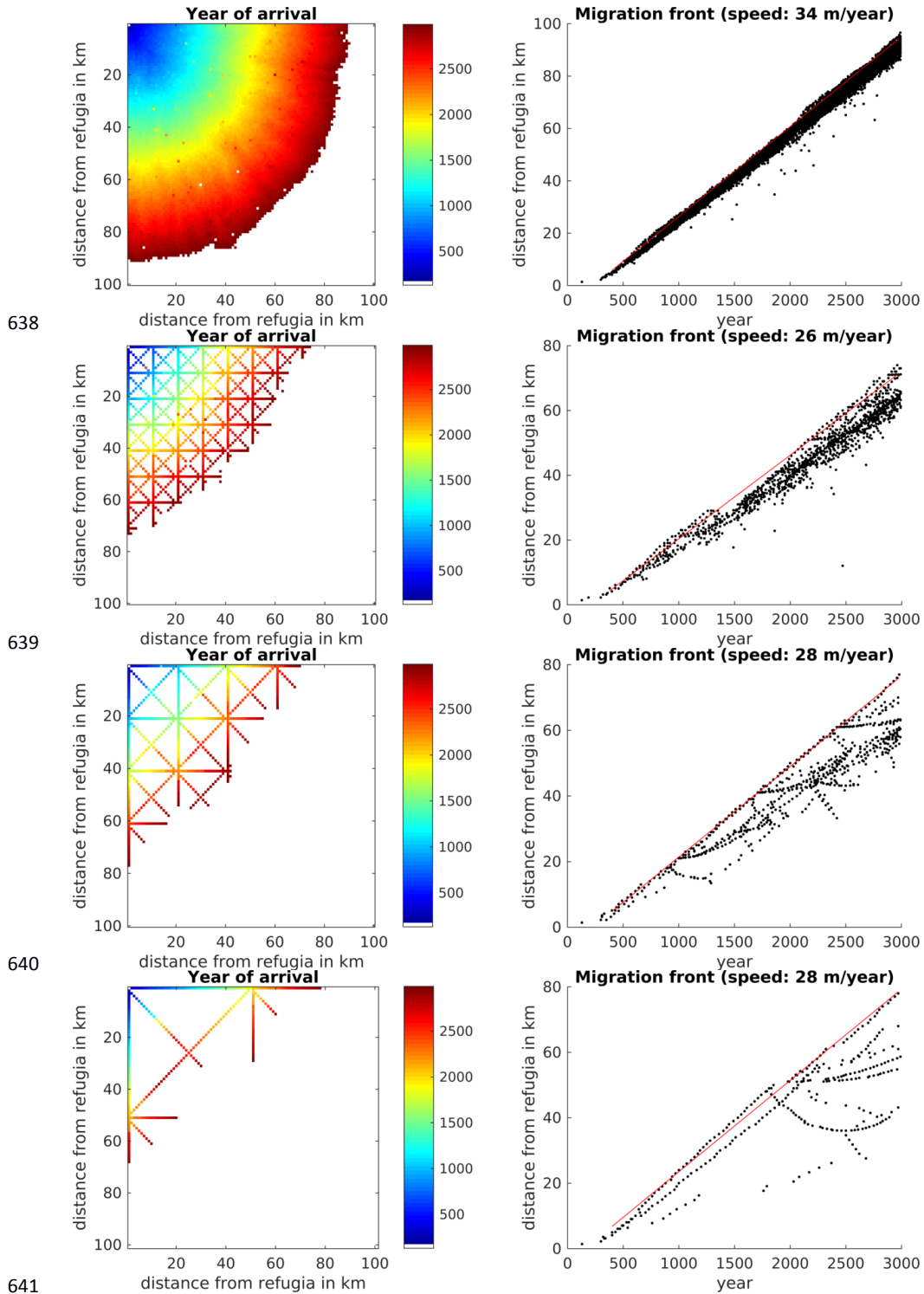
632



633

634 Fig. 2: Seed dispersal permeability for SMSM simulation tests. Each time the seed matrix is shifted,
635 the probability of entering the new cell (which in our test is set to $5 \cdot 10^{-7}$) is multiplied with the seed
636 dispersal permeability of the new potentially entered cell.

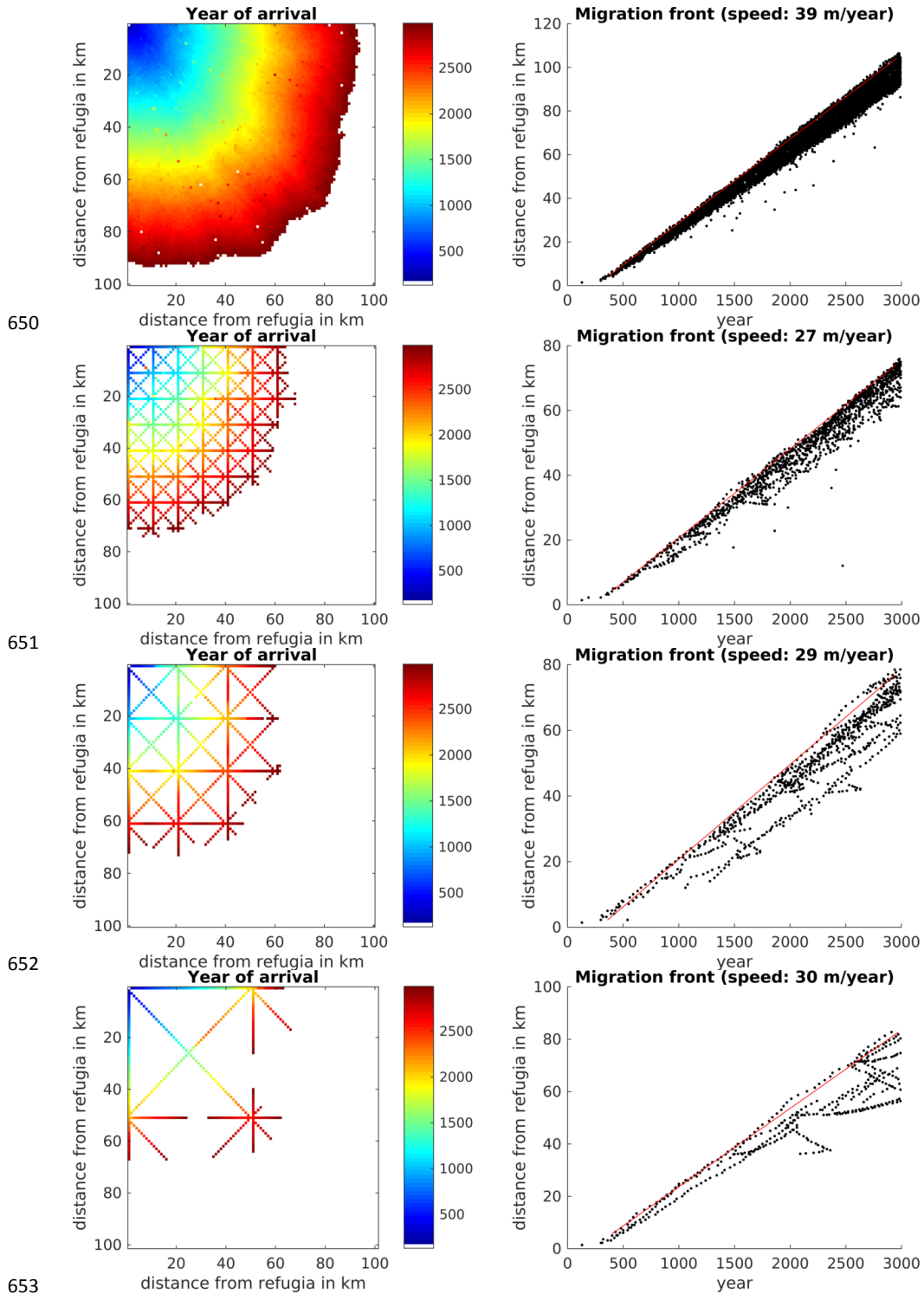
637





642 Fig. 3 Spread of *Fagus sylvatica* through an area of 100 * 100 grid cells with static climate using the
643 FFTM algorithm with no corridors or corridors every 10km, 20km or 50km. The left panels display
644 the time when *F. sylvatica* first reached an LAI of 0.5. *F. sylvatica* is allowed to establish freely only
645 in the upper left corner. The right panels show the distance of the grid cells with LAI 0.5 for *F.*
646 *sylvatica* from the starting point. The red line indicates the 95 percentile of the grid cells farthest away
647 from the starting point. The migration speed is calculated as slope of this line, taking only for grid
648 cells at least 5 km away from the starting point into account to avoid some initial establishing effects.

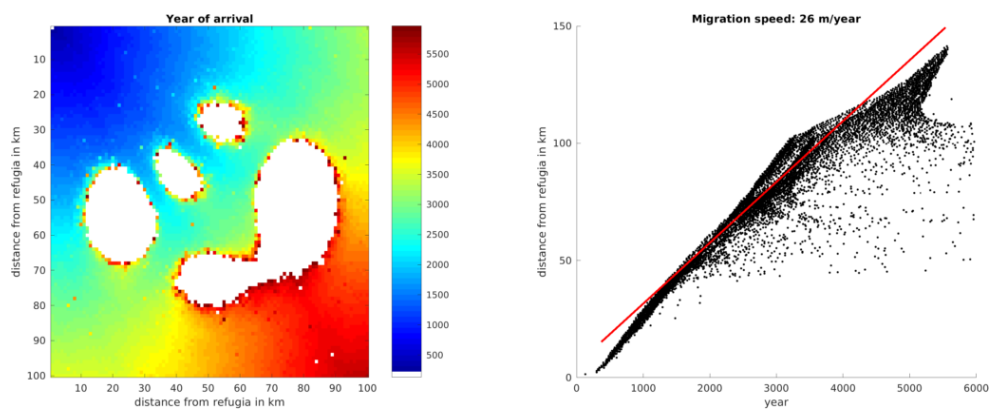
649





654 Fig. 4 Spread of *Fagus sylvatica* using the SMSM through an area of 100 * 100 grid cells with
655 identical climate, using the full area (upper row of panels) or corridors every 10th, 20th or 50th cell. For
656 more explanation see Fig. 3.

657



658

659 Fig. 5 Spread of *Fagus sylvatica* using the SMSM method through an area of 100 * 100 grid cells with
660 identical climate but probability of seed fall is set to 0.00005 multiplied with the spatially explicit seed
661 dispersal permeability value as shown in Fig. 2. Note that we increased the simulation time to 6000
662 years in order to have *F. sylvatica* establishing in all areas.

663



664 Table 1. Summary of migration speeds and calculation time. A corridor distance of 0 indicates no
 665 corridors but an area completely filled with grid cells. The simulated grid cells column lists the
 666 number of cells for which LPJ-GM calculates the population dynamics, in all simulations the
 667 simulation domain (for which the seed dispersal was calculated) had a size of 10000 grid cells and all
 668 simulations were performed over 3000 years. The last line lists a simulation identical to the others
 669 except that no seed dispersal was calculated to allow estimating the computation time demand for this
 670 operation.

Seed dispersal mode	Corridor distance (cells)	Simulated grid cells (corridor cells)	Migration speed, m/year	Computation time (cpu* h)	Comp. time change per corridor grid cell compared to sim. without dispersal (CPU h)	Total comp. time change for whole domain compared to sim. without dispersal (CPU h)	Percentage of CPU time for dispersal	Decrease due to corridor simulation
FFTM	0	10000	34	1800	+12%	+12%	11%	
FFTM	10	3330	26	650	+22%	-59%	18%	67%
FFTM	20	1765	28	400	+41%	-75%	29%	78%
FFTM	50	977	27	220	+41%	-86%	29%	88%
SMSM	0	10000	39	2000	+25%	+19%	16%	
SMSM	10	3330	27	700	+31%	-59%	19%	65%
SMSM	20	1765	29	400	+41%	-77%	23%	81%
SMSM	50	977	30	220	+41%	-86%	32%	89%
Non	0	10000	0	1600	0%	0%	0%	

671